Observer Based Detection of Sensor Faults In Wind Turbines

Peter Fogh Odgaard,
KK-electronic a/s, 8260 Viby J, Denmark, phone: +45 21744963 ; fax: +45 97211431; e-mail: peodg@kk-electronic.com

Jakob Stoustrup
Department of Electronic Systems, Aalborg University, 9220 Aalborg East, Denmark, email: jakob@es.aau.dk

Rasmus Nielsen & Chris Damgaard
KK-electronic a/s, 7430 Ikast, Denmark; email: ranie@kk-electronic.com & chdam@kk-electronic.com

Summary
An observer based scheme is proposed to detect sensor faults in wind turbines. In the example used for the proposed scheme the wind turbine drive train is considered. A model of the drive train is used to design the observer, and in this model the wind speed is an important input, however, if an unknown input observer the fault detection scheme can be non dependent on the actual wind speed. The scheme is validated on data from a more advanced and detailed simulation model. The proposed scheme detects the sensor faults a few samples after the beginning of the faults.

I. INTRODUCTION

As wind turbines increases in sizes and more wind turbine turbines are installed offshore the need for fast fault detection and accommodation increases. In many industrially manufactured wind turbines rather simple schemes are used to detect and accommodate faults. In this paper a three blade horizontal axis turbine is considered, which is controlled in a standard way with power optimization in partial load and speed control in full load mode.

In this paper an example on the fault detection and accommodation problem regarding the measurements around the drive train is considered. The rotor and generator rotational speed is almost always measured. Some designs even include two measurements of both to ensure redundancy, and fault detection could be based on a simple voting scheme. The drive train connects the rotor with the generator, and it could be modeled such that inputs to it are the aerodynamic torque and generator torque. The generator torque is measured/estimated in the converter and the aerodynamic torque can be estimated based on an estimate of the wind speed. The wind speed is estimated since the measurement is not very reliable.

Some examples can be found of fault detection and accommodation of wind turbines. An observer based scheme for detection of sensor faults for blade root torque sensors is presented in [1]. A residual based scheme is presented in [2] to detect and accommodate faults in wind turbines. Fault detection for electrical conversion systems can be found in [3, 4] and [5]

Due to the uncertainties of the wind speed measurements/estimates it would be beneficial to include some robustness towards these uncertainties in the detection scheme. This could e.g. be included if an unknown input observer, see [6], is used to generate fault residuals. An uncertain extra aerodynamic torque component can then be modeled as an unknown input. This scheme is subsequently applied to isolate sensor faults either being at one of the rotor speed sensors, the generator speed sensors or the generator torque measurements. In [7] this proposed scheme is presented and applied to set of different sensor faults resulting in fixed sensor values during the faults. In this paper the scheme is applied to a set of sensor faults in terms of a gain factor on the measurements.

First, the system is described, followed by a model of the wind turbine used for the fault detection. The subsequent section presents the proposed detection scheme and the design of it. A section of simulations presents how the scheme performs. The paper is finalized by a conclusion.

II. SYSTEM DESCRIPTION

The three blade horizontal axis turbine which is considered in this paper is controlled in the following way. In partial load of the wind turbine it is controlled to generate as much power as possible, this is achieved by keeping a specific ratio between the tip speed of the blades and the wind speed, which in turn is obtained by controlling the rotational speed through adjusting the converter torque. In the full power region the converter torque is kept constant and the rotational speed is adjusted by controlling the pitch angle of the blades which changes the aero-dynamical power transfer from wind to blades. This part of the wind turbine is illustrated in Fig. 1.

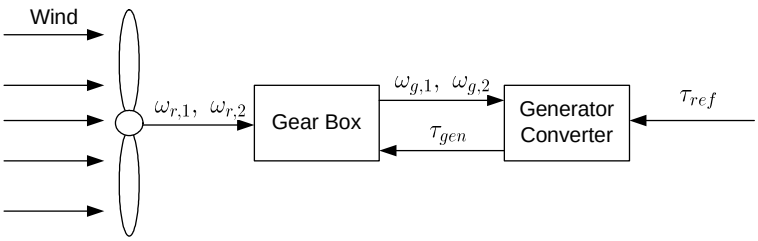

Fig. 1 Illustration of the principle of the wind turbine drive train. For illustrative purposes only two of the three blades are shown.

The wind turbine drive train in question has a number of measurements. $\omega_{r,1}[n]$ and $\omega_{r,2}[n]$ are two measurements of the rotor speed, $\omega_{g,1}[n]$ and $\omega_{g,2}[n]$ are two measurements of the generator speed, $\tau_{gen}[n]$ is the torque of the generator controlled by the converter which is provided with the torque reference, $\tau_{ref}[n]$. The estimated aerodynamic torque is defined as $\tau_{aero}[n]$. This estimate clearly depends on the wind speed, which unfortunately is very difficult to measure correctly. A very uncertain measurement is normally available which is used to provide 10 minutes mean values.

A. Model

The model is first defined in continuous time and subsequently transferred to discrete time.

The aerodynamic model is defined as in (1)

$$\tau_{\mathrm{aero}}(t) = \frac{\rho A C_{\mathrm{p}}(\theta(t), \lambda(t)) v^3(t)}{2\omega_{\mathrm{r}}(t)}, \tag{1}$$

Where ρ is the density of the air, A is the area covered by the turbine blades in its rotation, $\theta(t)$ is the pitch angle of the blades, $\lambda(t)$ is the tip speed ratio of the blade. (1) is used to estimate $\tau_{\mathrm{aero}}(t)$ based on an assumed estimated $v(t)$ and measured $\theta(t)$ and $\omega_{\mathrm{r}}(t)$. Due to the uncertainty of the estimate this could be considered as being unknown.

A simple one body model is used to represent the drive train, see (2).

$$\dot{\omega}_r(t) = \frac{1}{J}(\tau_{\mathrm{aero}}(t) - \tau_{\mathrm{gen}}(t)), \tag{2}$$

Where

$$\dot{\tau}_{gen}(t) = p_{gen}(\tau_{\mathrm{ref}}(t) - \tau_{\mathrm{gen}}(t)), \tag{3}$$

p_{gen} is the generator model parameter. This gives a simple state space model of the system, see (4)-(5).

$$\begin{bmatrix} \dot{\omega}_{\mathrm{r}}(t) \\ \dot{\tau}_{\mathrm{gen}}(t) \end{bmatrix} = \begin{bmatrix} 0 & -\frac{1}{J} \\ 0 & -p_{\mathrm{gen}} \end{bmatrix} \begin{bmatrix} \omega_{\mathrm{r}}(t) \\ \tau_{\mathrm{gen}}(t) \end{bmatrix} + \begin{bmatrix} \frac{1}{J} \\ 0 \end{bmatrix} \tau_{\mathrm{aero}}(t) + \begin{bmatrix} 0 \\ p_{\mathrm{gen}} \end{bmatrix} \tau_{\mathrm{ref}}(t), \tag{4}$$

$$\begin{bmatrix} \omega_{r,1}(t) \\ \omega_{r,2}(t) \\ \omega_{g,1}(t) \\ \omega_{g,2}(t) \\ \tau_{\mathrm{gen}}(t) \end{bmatrix} = \begin{bmatrix} 1 & 0 \\ 1 & 0 \\ N_r & 0 \\ N_r & 0 \\ 0 & 1 \end{bmatrix} \begin{bmatrix} \omega_r(t) \\ \tau_{gen}(t) \end{bmatrix}, \tag{5}$$

where N_r is the gear ratio. The parameters are chosen such that they represent a realistic turbine but not a specific one. The following parameters are used:

$\rho = 1.225 \frac{\mathrm{kg}}{\mathrm{m}^3},\ A = 6647.6\mathrm{m}^2,\ J = 7.794 \cdot 10^6 \mathrm{kg} \cdot \mathrm{m}^2,\ p_{\mathrm{gen}} = 100 \frac{1}{\mathrm{s}},\ N_r = 95,$

and the C_p table is chosen such that it represent an industrial turbine with blade diameter at 92 m.

Subsequently the continues model in (4)-(5) is discretized. This results in the following discrete time model.

$$\begin{bmatrix} \dot{\omega}_{\mathrm{r}}[n] \\ \dot{\tau}_{\mathrm{gen}}[n] \end{bmatrix} = \mathbf{A}_{\mathrm{d}} \begin{bmatrix} \omega_{\mathrm{r}}[n] \\ \tau_{\mathrm{gen}}[n] \end{bmatrix} + \mathbf{B}_{\mathrm{d}} \tau_{\mathrm{ref}}[n] + \mathbf{E}_{\mathrm{d}} \tau_{\mathrm{aero}}[n], \tag{6}$$

Where

$$\mathbf{A}_{\mathrm{d}} = \begin{bmatrix} 1.000 & -8.110 \cdot 10^{-10} \\ 0 & 0.3679 \end{bmatrix}, \tag{7}$$

$$\mathbf{B}_{\mathrm{d}} = \begin{bmatrix} -4.72 \cdot 10^{-10} \\ 0.6321 \end{bmatrix}, \tag{8}$$

$$\mathbf{E}_{\mathrm{d}} = \begin{bmatrix} 1.283 \cdot 10^{-9} \\ 0 \end{bmatrix}. \tag{9}$$

The output equation is:

$$\begin{bmatrix} \omega_{r,1}[n] \\ \omega_{r,2}[n] \\ \omega_{g,1}[n] \\ \omega_{g,2}[n] \\ \tau_{\text{gen}}[n] \end{bmatrix} = \begin{bmatrix} 1 & 0 \\ 1 & 0 \\ 95 & 0 \\ 95 & 0 \\ 0 & 1 \end{bmatrix} \begin{bmatrix} \omega_r[n] \\ \tau_{gen}[n] \end{bmatrix}, \quad (10)$$

III. METHOD

Due to the uncertainty of the estimation of τ_{aero} it would be preferable to introduce some robustness in the fault detection scheme. One could see the uncertainty as an unknown input signal; consequently an unknown input observer is an obvious choice, see [6]. If system is of the following form:

$$\mathbf{x}[n+1] = \mathbf{A}\mathbf{x}[n] + \mathbf{B}\mathbf{u}[n] + \mathbf{E}d[n], \quad (11)$$

$$\mathbf{y}[n] = \mathbf{C}\mathbf{x}[n], \quad (12)$$

where $d[n]$ is an unknown input, and $\mathbf{E}$ is the unknown input matrix.

The unknown input observer can be found as in (13)-(14).

$$\mathbf{z}[n+1] = \mathbf{F}_{n+1}\mathbf{z}[n] + \mathbf{T}_{n+1}\mathbf{B}_n\mathbf{u}[n] + \mathbf{K}_{n+1}\mathbf{y}[n], \quad (13)$$

$$\hat{\mathbf{x}}[n+1] = \mathbf{z}[n+1] + \mathbf{H}_{n+1}\mathbf{y}[n+1], \quad (14)$$

where $\mathbf{F}_{n+1}$, $\mathbf{T}_{n+1}$, $\mathbf{K}_{n+1}$ and $\mathbf{H}_{n+1}$are matrices designed to achieve decoupling from the unknown input and as well obtain an optimal observer. $\hat{x}$ is a vector of the states of the wind turbine model. The matrices in the unknown input observer are found using the following equation see (15)-(22), since system matrices are assumed constant these observer matrices are constant as well.

$$\mathbf{H} = \mathbf{E}(\mathbf{C}\mathbf{E})^{+}, \quad (15)$$

$$\mathbf{T} = \mathbf{I} + \mathbf{H}\mathbf{C}, \quad (16)$$

$$\mathbf{F} = \mathbf{A} - \mathbf{H}\mathbf{C}\mathbf{A} - \mathbf{K}^1\mathbf{C}, \quad (17)$$

$$\mathbf{K}^2 = \mathbf{F}\mathbf{H}, \quad (18)$$

$$\mathbf{K}^1 = \mathbf{A}^1\mathbf{P}\mathbf{C}^T\left(\mathbf{C}\mathbf{P}\mathbf{C}^T + \mathbf{R}\right)^{-1}, \quad (19)$$

$$\mathbf{A}^1 = \mathbf{A} - \mathbf{H}\mathbf{C}\mathbf{A}, \quad (20)$$

$$\mathbf{P} = \mathbf{A}^1\mathbf{P}^1(\mathbf{A}^1)^T + \mathbf{T}\mathbf{Q}\mathbf{T}^T + \mathbf{H}\mathbf{R}\mathbf{H}^T, \quad (21)$$

$$\mathbf{P}^1 = \mathbf{P} - \mathbf{K}^1\mathbf{C}\mathbf{P}(\mathbf{A}^1)^T, \quad (22)$$

The system states can subsequently be estimated by (13)-(14).

A. Residual generation

In order to generate the residuals for the fault detection and isolation system a residual $\mathbf{r}^i$ is computed for each sensor i using the unknown input observer scheme for a model where the ith sensor is removed from the C matrix and measurements, and define this matrix as $\mathbf{C}^i$, and the measurement vector from which the ith is removed is defined as $\mathbf{y}^i$. The observer for estimating $\mathbf{r}^i$ can be seen in (23)-(24).

$$\mathbf{z}[n+1] = \mathbf{F}^i\mathbf{z}^i[n] + \mathbf{T}^i\mathbf{B}\mathbf{u}[n] + \mathbf{K}^i\mathbf{y}^i[n], \quad (23)$$

$$\mathbf{r}^i[n] = (\mathbf{I} - \mathbf{C}^i\mathbf{H}^i\mathbf{y}^i[n] - \mathbf{C}^i\mathbf{z}^i[n], \quad (24)$$

The matrices $\mathbf{F}^i$, $\mathbf{T}^i$, $\mathbf{K}^i$, $\mathbf{H}^i$, are found as in (15)-(22) with the only difference that $\mathbf{C}$ is replaced with $\mathbf{C}^i$. The residual vector consists of some elements defined as, in this case with 5 sensors:

$$\mathbf{r}^i[n] = \begin{bmatrix} r_1^1 \\ r_2^i \\ r_3^i \\ r_4^i \end{bmatrix}, \quad (25)$$

These computed residuals are subsequently used to compute the actual detection signal. Define the detection signal for the five sensors as: $\kappa_{\omega_{r,1}}$, $\kappa_{\omega_{r,2}}$ as the two rotor angular speed detection signals, $\kappa_{\omega_{g,1}}$, $\kappa_{\omega_{g,2}}$, and κ_{τ_g} as the generator torque detection signal. These detection signals are computed as in (26)-(30):

$$\kappa_{\omega_{r,1}}[n] = r_1^2[n] \cdot r_1^3[n] \cdot r_1^4[n] \cdot r_1^5[n], \quad (26)$$
$$\kappa_{\omega_{r,2}}[n] = r_1^1[n] \cdot r_2^3[n] \cdot r_2^4[n] \cdot r_2^5[n], \quad (27)$$
$$\kappa_{\omega_{g,1}}[n] = r_2^1[n] \cdot r_2^2[n] \cdot r_3^4[n] \cdot r_3^5[n], \quad (28)$$
$$\kappa_{\omega_{g,2}}[n] = r_3^1[n] \cdot r_3^2[n] \cdot r_3^3[n] \cdot r_4^5[n], \quad (29)$$
$$\kappa_{\tau_g}[n] = r_4^1[n] \cdot r_4^2[n] \cdot r_4^3[n] \cdot r_4^4[n], \quad (30)$$

A sensor fault is present at the ith sensor if

$$|\kappa_i[n]| > \gamma_i \cdot \kappa_i^{\max}, \quad (31)$$

Where γ_i is the threshold of the ith fault residual, and $\kappa_i^{\max}$ is the recorded maximal value of the κ_i. The values of these thresholds are found tests on the simulated data, such that false positive detections are avoided while the sensor fault is still detected as fast as possible. The values are specified as:

$$\gamma_1 = 0.05,\ \gamma_2 = 0.05,\ \gamma_3 = 0.4,\ \gamma_4 = 0.4,\ \gamma_5 = 0.5$$

IV. SIMULATIONS

The simulations are performed on a simulation model of the drive train in which measurement noises are added to the measurements. In addition a two body model is used to represent the drive train itself instead of the one body mode used to design the observer. In this example the wind is varying between 7m/s and 13 m/s meaning that in this simulation, the turbine runs in partial load, and consequently the pitch angle is constant at 0 deg, and $\tau_{ref}[n]$ is controlled to keep the optimal tip speed ratio. Measurement noises are added to all sensors with the following variances: $\sigma_{\omega_r} = 1 \cdot 10^{-3},\ \sigma_{\omega_g} = 2.5 \cdot 10^{-4},\ \sigma_{\tau_{gen}} = 8100$. These variances are in the same order as experimental found values on a wind turbine similar to the turbine represented by this simulation model.

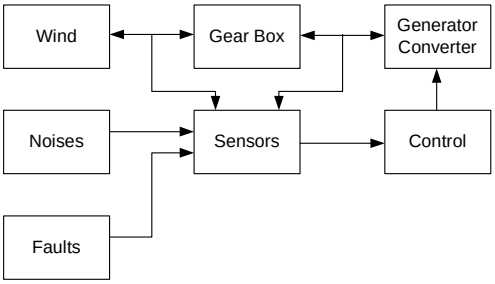

Fig. 2 Illustration of the blocks in the simulation model.

Sensor faults are simulated by scaling the sensor output for a period of 500 samples (5s). The scale values are found according to the absolute values such that the amplitude of the fault is realistic. The rotor and generator speed sensors are scaled with a factor of 0.7 and the converter torque measurement is scale with a factor of 0.8. In the following figure, normed residuals for each sensor are plotted together with the detection thresholds. All detection signals (κ) can be seen in Fig. 3.

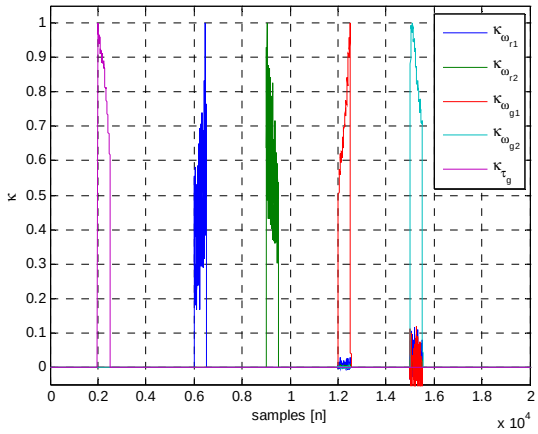

Fig. 3 the five κ signals plotted together to show the time location of the five different sensor faults.

A. Fault in rotor speed sensor #1

$\omega_{r,1}[n]$ has a fault from sample 6000 to sample 6500, and as the plot of the residual compared with the threshold shows, now false positive detections are present, see Fig. 4.

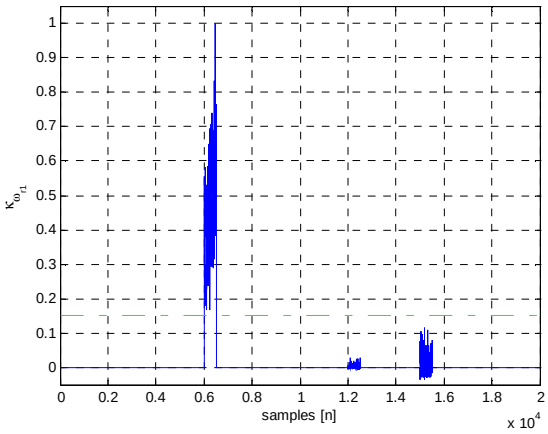

Fig. 4 Fault residual for $\omega_{r,1}[n]$, the fault is detected during its presence.

A zoom on the beginning and end of $\kappa_{\omega_{r,1}}$ can be seen in Fig. 5 from which it can be seen that the fault is detected from sample 6002 to sample 6502. This means that this sensor fault can be detected quite fast without any false positive detections.

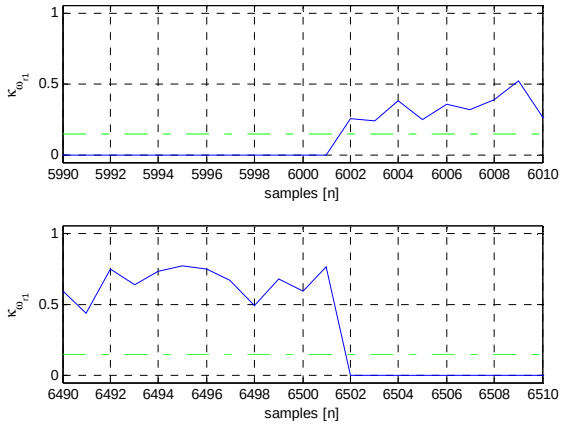

Fig. 5 A zoom on $\kappa_{\omega_{r,1}}$ during the beginning and end of the sensor fault.

B. *Fault in rotor speed sensor #2*

$\omega_{r,2}[n]$ has a fault from sample 9000 to sample 9500, and as the plot of the residual compared with the threshold shows that the fault is detected without any false positive detections, see Fig. 6. In order to find the detection times of this fault, a zoom is made on the beginning and ends of the fault. This plot can be seen in Fig. 7, from which it can be seen that the fault is detected from sample 9002 to sample 9502, which again results in fast detection of the fault.

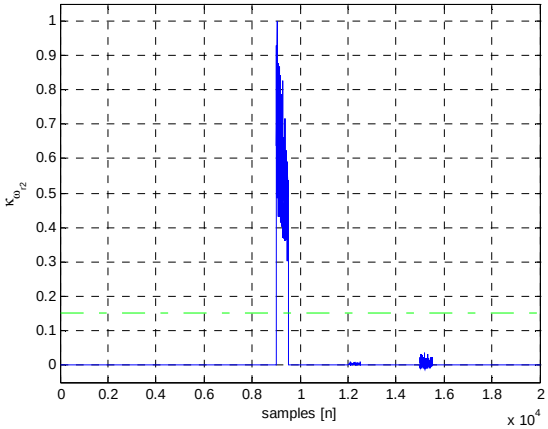

Fig. 6 Fault residual for $\omega_{r,2}[n]$, the fault is detected during its presence.

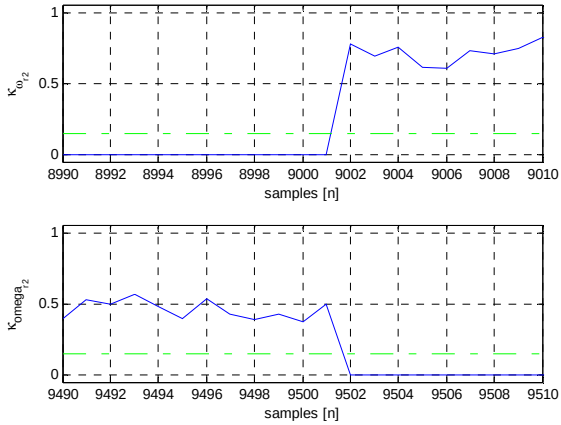

Fig. 7 A zoom on $\kappa_{\omega_{r,2}}$ during the beginning and end of the sensor fault.

C. *Fault in generator speed sensor #1*

A sensor fault is present in $\omega_{g,1}[n]$ from sample 12000 to sample 12500. Using the found threshold this sensor fault is detected without any false positive detections, even though it contains strong reactions on the other generator speed sensor fault. This is due to the specific measurement noise sequence in use in this simulation, see Fig. 8. Inspecting a zoom on the beginning and end of this specific sensor fault, it can be seen that this fault is detected from sample 12005 to 12502, see Fig. 9.

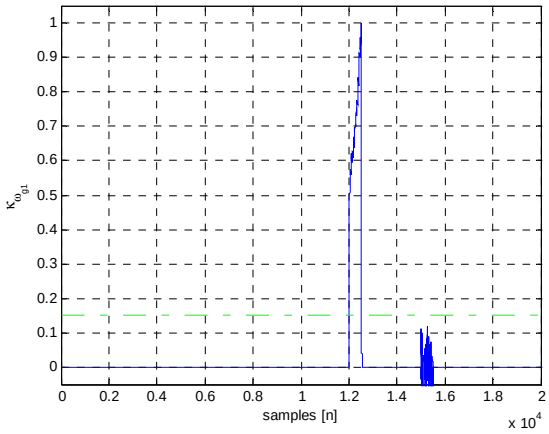

Fig. 8 Fault residual for $\omega_{g,1}[n]$, the fault can be detected during its presence.

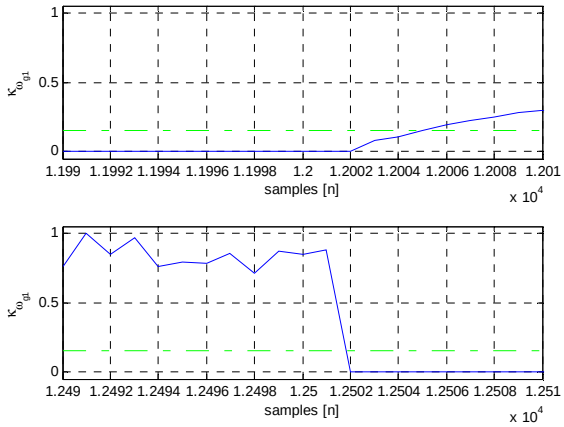

Fig. 9 A zoom on $\kappa_{\omega_{g,1}}$ during the beginning and end of the sensor fault.

D. Fault in generator speed sensor #2

A sensor fault in $\omega_{g,2}[n]$ is present from sample 15000 to sample 15500. From Fig. 10 it can be seen that this sensor fault is detected without any false detections, and with significantly less influence from $\omega_{g,1}$ than $\kappa_{\omega_{g,1}}$ was influenced by $\omega_{g,2}$. The reason is as mentioned in Section IV.C related to the specific measurement noise sequences used in the simulation. The fault is detected from sample 15003 to 15502, see Fig. 11.

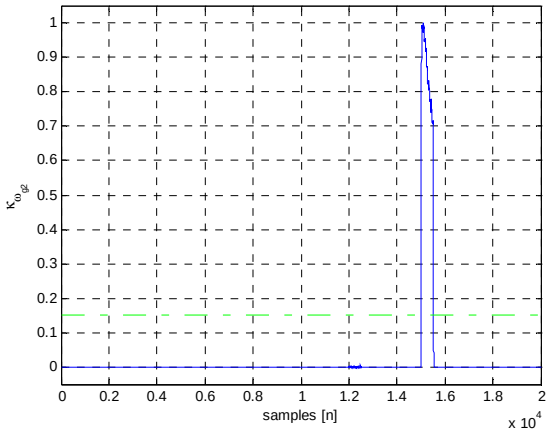

Fig. 10 Fault residual for generator speed measurement no. 2, the fault is detected during its presence.

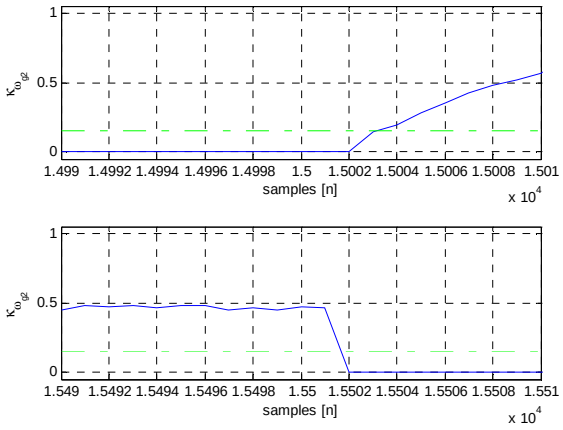

Fig. 11 A zoom on $\kappa_{\omega_{g,2}}$ during the beginning and end of this sensor fault.

E. Fault in converter torque measurement

The sensor fault is present in the torque measurement from sample 2000 to sample 2500. Fig. 12 shows that a threshold can be chosen such that false positive detections can be avoided. In Fig. 13 a zoom on $\kappa_{\tau_{gen}}$ is provided for the beginning and end of the fault to determine the detection times of these. It can be seen that the beginning of the fault is detected at sample 2002 and that the end is detected at sample 2502.

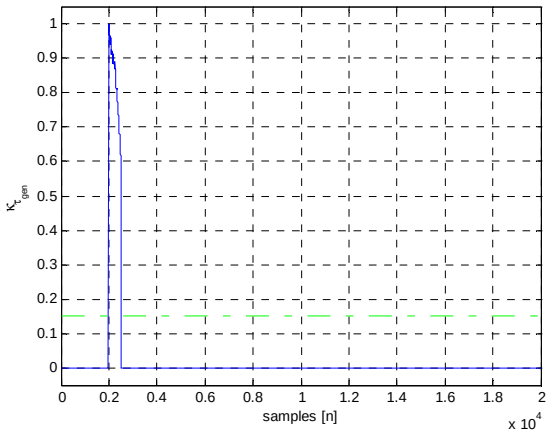

Fig. 12 Fault residual for the generator torque. .

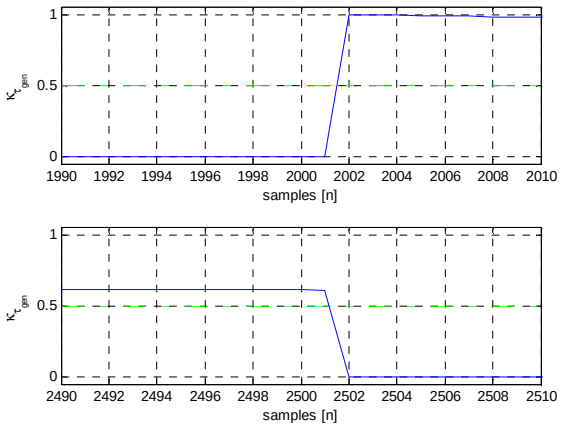

Fig. 13 A zoom on $\kappa_{\omega_{g,2}}$ during the beginning and end of this sensor fault.

V. CONCLUSION

In this paper an unknown input observer is designed to detect five different sensor faults in the drive train of a three blade horizontal axis wind turbine. Since the wind speed is uncertain, it is considered as being an unknown input in the observer design. A simple one-body model is used of the gear box in the observer model, whereas the system is simulated with a more detailed two-body model for simulating the sensor faults. The observer based detection and isolation scheme detects all five sensor faults within a few samples after the occurrence of them, without any false positive detections.

REFERENCES

[1] X. Wei, M. Verhaegen, and T. van den Engelen, "Sensor fault diagnosis of wind turbines for fault tolerant," in *Proceedings of the 17th World Congress The International Federation of Automatic Control*. Seoul, South Korea: IFAC, July 2008, pp. 3222–3227.

[2] C. Dobrila and R. Stefansen, "Fault tolerant wind turbine control," Master's thesis, Technical University of Denmark, Kgl. Lyngby, Denmark, 2007.

[3] K. Rothenhagen and F. Fuchs, "Current sensor fault detection and reconfiguration for a doubly fed induction generator," in *Proc. IEEE Power Electronics Specialists Conference PESC 2007*, F. Fuchs, Ed., 2007, pp. 2732–2738.

[4] K. Rothenhagen, S. Thomsen, and F. Fuchs, "Voltage sensor fault detection and reconfiguration for a doubly fed induction generator," in *Proc. IEEE International Symposium on Diagnostics for Electric Machines, Power Electronics and Drives SDEMPED 2007*, S. Thomsen, Ed., 2007, pp. 377–382.

[5] P. Poure, P. Weber, D. Theilliol, and S. Saadate, "Fault-tolerant power electronic converters: Reliability analysis of active power filter," in *Proc. IEEE International Symposium on Industrial Electronics ISIE 2007*, P. Weber, Ed., 2007, pp. 3174–3179.

[6] J. Chen and R. J. Patton, *Robust model-based fault diagnosis for dynamic systems*, 1st ed. Kluwer academic publishers, 1999.

[7] P. F. Odgaard, J. Stoustrup, C. Damgaard, and R. Nielsen, "Observer based fault detection of sensor faults in wind turbine drive train," September 2008, submitted for publication.